Macromolecules
ARTICLE

Macromolecules **2009**, *42*, 7919–7923 **7919**
DOI: 10.1021/ma9013498

Dewetting of PMMA on PS−Brush Substrates

Bokyung Kim and Du Yeol Ryu*

Department of Chemical Engineering, and Active Polymer Center for Pattern Integration, Yonsei University, Seoul 120-749, Korea

Victor Pryamitsyn and Venkat Ganesan*

Department of Chemical Engineering, University of Texas at Austin, Austin, Texas 78712

Received June 23, 2009; Revised Manuscript Received September 3, 2009

ABSTRACT: We present experimental results quantifying the dewetting behavior of poly(methyl methacrylate) (PMMA) melt on polymer brushes of polystyrene (PS) molecules. Our studies indicate contact angles which display a brush molecular weight dependence similar to that expected for autophobic dewetting situation. We use strong segregation theory calculations to model the interfacial tension behavior in our observations and delineate the interplay between enthalpic and entropic effects in polymer wetting upon polymer brushes.

Grafting polymer molecules onto surfaces (to form polymer brushes) has become a common procedure to precisely tune the surface properties such as adhesion, lubrication, slip, and the wettability of the surfaces. At high coverages, the grafted polymer chains optimize between the energetic costs of crowding and stretching to adopt a conformation that is stretched in the direction normal to the grafting surface.[1,2] Because the latter conformations are quite different from the random coil configurations exhibited by linear polymer molecules in bulk, the properties of polymer brushes are also usually significantly different from bulk polymers.[3−5]

The wetting behavior of polymers on polymer brushes is a property where the above-mentioned differences between bulk and brush behaviors are most transparent. The case that has been widely studied, termed autophobic dewetting, refers to the wetting characteristics of a polymer on a polymer brush *of the same chemical identity* (or a copolymer strongly adhered to substrate).[6−16] In this situation, enthalpic effects are absent, and the overall behavior is driven by entropic effects. In such a case, the polymer may either mix (wet), partially wet, or dewet (segregate from) the brush depending on the ratio of molecular weights of the components and the grafting density of the brush. Because of the important ramifications in the context of surface adhesion applications, these features have constituted the focus of many earlier experimental and theoretical researches.[17−21]

In contrast, the wetting characteristics of polymers which are chemically different from the brush component has attracted far less attention but has a number of practical ramifications in the context of designing functionalizers for dispersion of particles in polymers.[22,23] In this article, we report the wetting properties of a model system of poly(methyl methacrylate) (PMMA) on polymer brushes of polystyrene (PS) molecules. The molecular weights (chain lengths) of both polymers were varied and the contact angles of PMMA droplets were measured. We find that even in this system of immiscible polymers, the entropic wetting features characteristic of autophobic dewetting persists up to very large molecular weights of the components. We demonstrate that the experimental results can be qualitatively modeled by strong segregation theory and scaling arguments and use the latter to shed light on the parametric interplay between enthalpic and entropic effects in the interfaces between polymers and polymer brushes.

*To whom correspondence should be addressed. For D.Y.R., E-mail, dyryu@yonsei.ac.kr. For V.G.: E-mail, venkat@che.utexas.edu.

1. Experimental Section

A. Materials and Methods. Poly(methyl methacrylate) (PMMA) was synthesized by the anionic polymerization of methyl methacrylate in tetrahydrofuran (THF) containing excess LiCl (high purity, Aldrich) at −78 °C under purified argon using an initiator prepared by *sec*-butyllithium addition to 1,1-diphenylethylene. Number-average molecular weights (M_n) and polydispersity (M_w/M_n) of PMMAs were characterized by size-exclusion chromatography (SEC) with the multiangle laser light scattering (MALLS), respectively. Hydroxyl-terminated polystyrene (PS−OH) with the various chain lengths was synthesized via anionic polymerization (polymer source) to prepare PS-brushed substrates. PS chains can be anchored to the Si substrate by spin coating a film of PS−OH from toluene solution then thermal annealing thin film at 170 °C under vacuum for 3 days, well above the glass transition temperatures (T_g) of PS. The nonanchored chains were completely removed by rinsing with toluene. The film thickness of PS brush was measured by ellipsometry (Nanoview Co.). The characteristics of PS-brushed substrates in this study are listed in Table 1.

The "graft-to" method was used to graft functional PS homopolymers onto the surface of the standard Si substrates. The end-hydroxyl groups of hydroxyl polystyrene (PS−OH) diffuse to and react with the native oxide layer of PS, thereby producing PS brushes to the substrate. The complete sequential procedure for the experiments is illustrated in Figure 1. We controlled the thickness (or height) of PS brushes as well as the grafting densities by adopting the various molecular weights of PS−OH, ranging 1600 to 38000 g/mol, which lead to the brush thicknesses ranging from 2.2 to 13.2 nm.

The film thickness of PMMA was controlled to be 20 nm on the PS−brush substrates. For thermal equilibrium at interfaces, the PMMA thin films were again set to 170 °C as an annealing temperature under vacuum for 3 days, which is much higher than the glass transition temperatures (for bulk and thin films) of PS and PMMA.[24−26] Scanning force microscopy (SFM; Dimension 3100, Digital Instrument Co.) was operated in the tapping mode to measure the static contact angles of dewetting

Published on Web 09/17/2009

Table 1. Characteristics of PS−Brush Substrates in This Study

sample code	M_n	M_w/M_n	brush thickness (nm)	R_g[a] (nm)	grafting density, σ (chains/nm^2)[b]	d_g[c] (nm)
PSOH-02	1600	1.08	2.2	1.095	0.877	1.205
PSOH-04	3700	1.08	4.4	1.666	0.743	1.309
PSOH-06	6000	1.07	5.8	2.121	0.61	1.445
PSOH-10	10000	1.05	9.3	2.739	0.585	1.476
PSOH-14	14000	1.09	11.1	3.24	0.499	1.598
PSOH-20	19500	1.05	12.8	3.824	0.414	1.753
PSOH-38	38000	1.09	13.2	5.339	0.219	2.411

[a] Radius of gyration calculated by assuming linear PS chains. [b] The grafting density of PS brushes were calculated using $\sigma = \rho d_0 N_A/M_n$, where d_0 represents the brush height, the mass density of PS is denoted as ρ (1.05 g/cm^3), N_A and M_n represent the Avogadro's number and the number-average molecular weights of PS−OH respectively. [c] The average distance between the grafting points was calculated using $d_g = 2/(\sigma\pi)^{1/2}$.

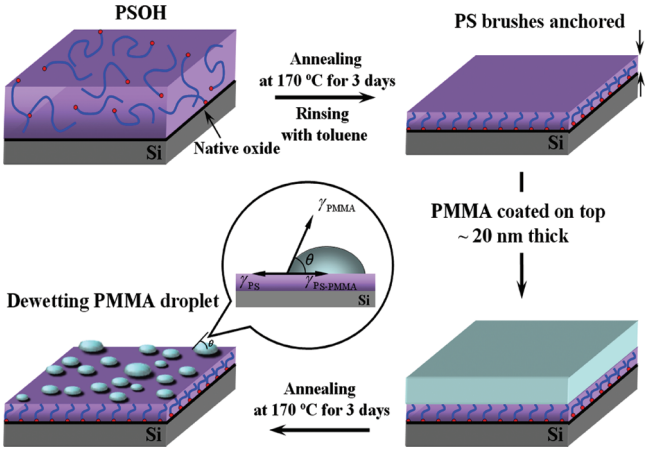

Figure 1. Scheme for the experimental procedure in this study.

PMMA droplets from the surface topology in nanometer scale. The hemispherical PMMA droplets appearing brighter in height and phase due to the viscoelastic contrast between the PMMA and PS components.

B. Results. Figure 2 displays the height and the calculated grafting density σ for the resulting PS−brushes. The grafting density was calculated using:

$$\sigma = \rho d_0 N_A/M_n \quad (1)$$

where d_0 represents the brush height, the mass density of PS is denoted as ρ (1.05 g/cm^3), and N_A and M_n represent the Avogadro's number and the number-average molecular weights of PS−OH, respectively. The height of the resulting brushes (afterrinsing with toluene), measured as a function of the molecular weight of PS−OH, is seen to increase to 13 nm for 20000 g/mol, and then remains almost constant for higher molecular weights of PS−OH. By repeating the experiments at a higher temperature (>170 °C), we verified that the annealing temperature has negligible influence on the results presented. Therefore, the plateauing of the brush heights noted for higher molecular weights of PS−OH is unlikely due to temperature annealing effects and is more likely due to the low concentrations of the end-hydroxyl groups and the low diffusivities of high molecular weight PS−OH, which hinders the grafting process. Interestingly, a macroscopic surface property (hydrophilicity or hydrophobicity) of the PS−brushes when assessed by the contact angle for water showed a value of 92 ± 3° consistently regardless of the brush thicknesses, indicating that even the ultrathin brush thicknesses of 2.2 nm constitutes an efficient coverage of the native oxide substrate (presumably due to the highest grafting density 0.877chains/nm^2).[27]

The PMMA films were spin-coated on the various PS-brushed substrates, followed by thermal annealing at 170 °C

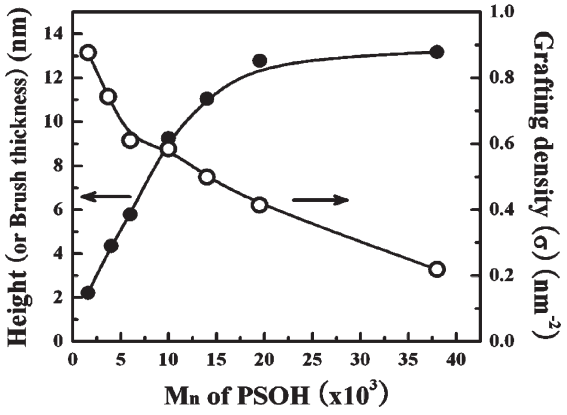

Figure 2. Brush thickness (heights) and the (calculated) grafting densities of PS−OH brushes as a function of the molecular weights of the grafted polymer.

under vacuum for 3 days to equilibrate thin films at interfaces. The PMMA films dewet on the brush substrates in a hemispherical shape, as shown in Figure 1. The contact angles for the PMMA droplets were then obtained using:[28]

$$\tan(\theta/2) = H/R \quad (2)$$

(valid for $\theta < 90°$) where H and R denote height and radius of the droplets, respectively.

Parts a and b of Figure 3 present the main experimental results of this letter. In Figure 3a, we present the results for the contact angles for PMMA on a specific PS−brush substrate as a function of the molecular weight of PMMA. Shown also are images of the dewetting PMMA droplets obtained by the distance profiling across the centers using scanning force microscopy (SFM). Figure 3b presents results for the contact angle values of PMMA of different molecular weights on brushes of different heights. For a brush of specified thickness, the contact angles are seen to increase with increasing PMMA molecular weight and then plateaus around a molecular weight of 20000 g/mol. On the other hand, for a specific molecular weight of PMMA, it is observed that the contact angles for PMMA are the highest at the thinnest PS−brushes and they monotonically decrease with increasing brush thickness. We note that these contact angles for PMMA decreased by approximately 8° when the samples were annealed at 210 °C (not shown here), indicating that the interfacial energies do exhibit a temperature dependence.

C. Discussion. We note that the contact angle θ between PMMA and PS is related to the interfacial tensions between PS−air (γ_{PS-air}), PMMA−air ($\gamma_{PMMA-air}$), and PS−PMMA ($\gamma_{PS-PMMA}$) through:[29]

$$\cos\theta = (\gamma_{PS-air} - \gamma_{PS-PMMA})/\gamma_{PMMA-air} \quad (3)$$

If we assume that $\gamma_{PMMA-air}$ and γ_{PS-air} display only weak molecular weight dependencies (as is true for interfacial tensions of strongly segregated polymer−solvent systems[30]), it is evident that the results displayed in Figure 3 should mirror the trends exhibited by $\gamma_{PS-PMMA}$. To shed light on our experimental observations, we first compare the trends displayed in Figure 3 to situations for which there exists a theoretical understanding of interfacial tension between polymers.

For the interfaces between two incompatible polymer *melts* of different molecular weights, the interfacial tension has been theoretically calculated as:[30]

$$\gamma_{melt-melt} \propto \sqrt{\chi}\left[1 - \frac{\pi^2}{12}\left(\frac{1}{\chi N_A} + \frac{1}{\chi N_B}\right)\right] \quad (4)$$

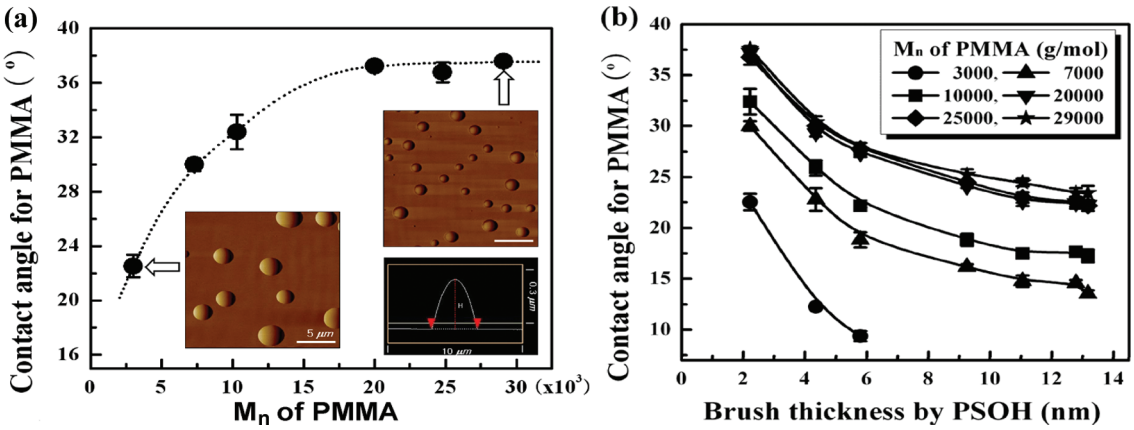

Figure 3. (a) Contact angles for PMMA on the PS−brush substrates as a function of the molecular weight of PMMA, where the insets show SFM phase images for dewetting PMMA droplets of M_n = 3000 and 29000 g/mol and a distance profiling in a SFM height image. The molecular weight of PS and brush thickness are 1600 g/mol and 2.2 nm, respectively. (b) Contact angles of the PMMA droplets of different molecular weights on PS−OH brushes of varying thicknesses.

where χ denotes the Flory−Huggins interaction parameter between the immiscible components and N_A and N_B are the number of segments in the polymers. In contrast, for *melt−brush interfaces*, explicit analytical models for the interfacial tension do not exist even for the autophobic case of chemically identical polymers. However, scaling theories have been developed for the so-called dry-brush regime of the interpenetration of a polymer inside a brush of identical chemical identity. Explicitly, Leibler et al. predicted that for infinitely long melt polymers, the interfacial tension, $\gamma_{melt-brush}$ should scale as $\sigma^{1/3}$.[20,23] They also suggested that for finite molecular weights of the melt polymer, $\gamma_{melt-brush}$ should decrease either upon lowering the molecular weight of the melt or increasing the molecular weight of the brush and eventually transitions to a case where the melt polymer wets the brush.

How do the results of Figure 3 compare with the above theoretical predictions? It is apparent by comparing to the expression 4 that our results do not match the behavior expected for interfacial tension between incompatible polymer melts. Indeed, in such a case, increasing the molecular weight of the brush polymer should lead to an increase in the overall interfacial tension and eventually transition to its asymptotic value corresponding to very long polymers. Our experimental results follow an opposite trend where they decrease with an increase in the molecular weight (and height) of the brush component. On the other hand, we observe that our experimental results does qualitatively match the trends predicted for the (entropically driven) autophobic melt−brush regime. Indeed, in such a case, an increase in the molecular weight of the brush polymer should lead to a lowering of the melt−brush interfacial tension and eventually transition to a completely wetting behavior.

While the above discussion suggests that the physics underlying Figure 3 is likely the same as that for the entropically driven interfacial tensions between chemically identical polymers, few issues still remain to be clarified. One issue is the influence of chemical incompatibility upon the interfacial tension between melt polymers and incompatible polymer brushes. A second issue relates to the reasoning that in the limit of small interfacial thickness between the melt and the brush, one may expect that the fact that one of the chains is grafted should not matter and the structure and energetics of the melt−brush interface should resemble the characteristics of the melt−melt interface. An interesting question is "in which parametric regime does this transition to a melt−melt like interface occur?" To resolve these issues, in the next section we present the results of calculations based on strong segregation theory for the characteristics of the interfaces between chemically dissimilar melt and brush polymers.

2. Strong Segregation Theory

Strong segregation theory (SST) has played an important role in the fundamental understanding of the structure and energetics of polymer−brushes and polymer−melt interfaces.[20,31] While the accuracy of SST may not match that of polymer self-consistent field theories (SCFT), the implementation and the numerical details of SST are usually substantially simpler than SCFT. Moreover, several pioneering numerical studies by Matsen has indicated that the qualitative behavior of density profiles, free energies, etc. are in most cases well-captured by strong segregation theory.[21,32−34]

We adopt the strong segregation theory (SST) presented by Semenov for the case of an incompressible system of melt polymer in contact with a polymer brush.[20,31] We start with the expression for the free energy F per unit area of a film of thickness d containing a polymer brush (of N segments) with a grafting density σ in contact with a homopolymer melt with polymers containing P segments. We use nondimensional variables, with all the distances normalized by the unperturbed radius of gyration of the brush chain, $R_g \equiv b(N)^{1/2}/(6)^{1/2}$. We use $\phi_b(z)$ to denote the volume fraction profile of the brush polymer segments. In this representation,

$$\frac{FN}{\rho_0 R_g} = \int_0^d \mathrm{d}z \left[\frac{\pi^2}{16} z^2 \phi_b(z) + \frac{1}{4} \frac{(\mathrm{d}\phi_b/\mathrm{d}z)^2}{\phi_b(1-\phi_b)} + \frac{(1-\phi_b)\ln(1-\phi_b)}{\alpha} + \chi N \phi_b(1-\phi_b) \right] \quad (5)$$

(ρ_0 denotes the monomeric volume of the polymer, which has been assumed to be the same for both the brush and melt polymers.) In eq 5, the first term represents the stretching energy of the polymer brush, whereas the second and third term quantifies respectively the entropic contributions arising from the density variations of the polymers and the translational degrees of the homopolymer (with $\alpha \equiv P/N$). The last term represents the enthalpic interaction term. The above is subject to the constraint of grafting density:

$$\int_0^d \mathrm{d}z \phi_b(z) = \tilde{\sigma} \quad (6)$$

where $\tilde{\sigma} = \sigma R_g^2/(\rho_0 R_g^3/N)$. Paranthetically, we note that the case of "autophobic dewetting" is an instance where the approximations embodied in the above strong segregation theory proves to be

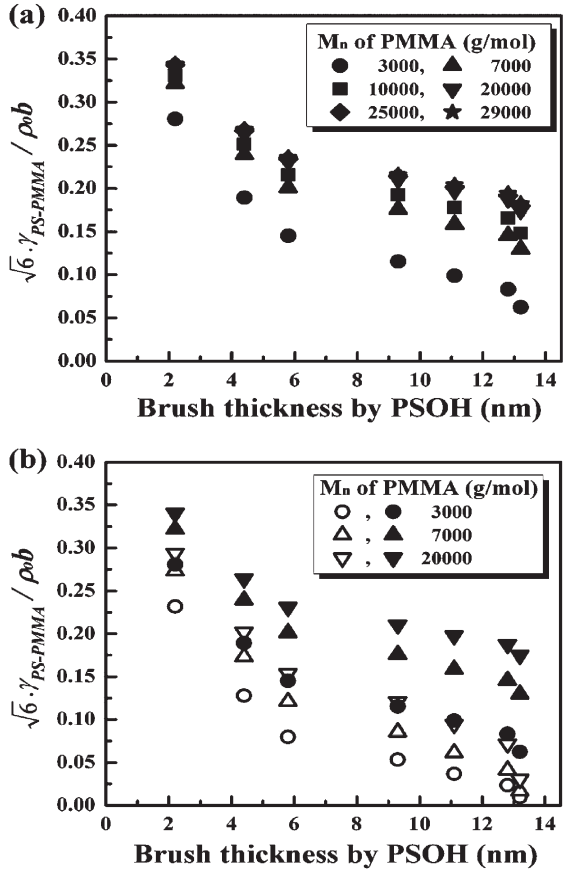

Figure 4. (a) Results for $\gamma_{PS-PMMA}$ calculated from SST. (b) Comparison of $\gamma_{PS-PMMA}$ calculated from SST for the case of $\chi \equiv \chi_{PS-PMMA} = 0.037$ (closed symbols)[35] with the "autophobic" case (open symbols) for which $\chi = 0$.

quantitatively inadequate.This inaccuracy has been carefully investigated by Matsen[34] and has been linked to the square-gradient term in eq 5. In this article, because our intent is to seek some qualitative insights into the experimental results, we rely on the simple version of the strong segregation theory embodied in eq 5.

To find the equilibrium density profiles and the free energies for a given thickness d, we numerically minimize the above functional (eq 5) subject to the constraint of grafting density (eq 6) for the specific experimental parameter values $\tilde{\sigma}$, N, P, and χN. The interfacial tension, $\gamma_{PS-PMMA}$ is obtained by finding the free energy (per unit area) difference between an infinitely thick film and a film for which the free energy is minimum.[20,29]

The interfacial tension values so determined are displayed in Figure 4a. It is observed that there is an agreement between the trends exhibited by the experimental results for the contact angles (Figure 3) and the numerical results for $\gamma_{PS-PMMA}$. Specifically, we observe that for a brush of specified thickness, the interfacial tensions increases with increasing PMMA molecular weights, eventually plateauing at higher molecular weights. On the other hand, for a specific molecular weight of PMMA, it is observed that the interfacial tensions are the highest at the thinnest PS−brushes and they monotonically decrease with increasing brush thickness. Both these features are consistent with the experimentally noted behaviors for the contact angles.

An interesting question pertains to the role of the chemical incompatibility in influencing $\gamma_{PS-PMMA}$. To shed light on this issue, in Figure 4b, we compare our results for $\gamma_{PS-PMMA}$ (for which $\chi = 0.037$[35]) with those obtained for a system of *athermal* ($\chi = 0$) melt and brush polymers wherein all other parameters were kept the same. The latter case corresponds to the widely studied situation of autophobic wetting behavior. It can be observed from our results that the trends observed for $\gamma_{PS-PMMA}$ (and the contact angles) in our experiments on incompatible polymers are qualitatively similar to the behavior for the chemically identical athermal situation. Consequently, we deduce that the incompatibility effects are seen to only influence the quantitative values of the interfacial tensions while retaining the qualitative trends observed for chemically identical polymers.

While the above results suggests that the experimental observations on dewetting of PMMA on PS can be rationalized qualitatively by the physics of interfacial tension between a brush and chemically distinct polymer, it is of interest to query whether in certain parametric ranges the interfacial characteristics ever start to resemble the behavior expected for interfaces between incompatible melts (cf. eq 4). To discern this, we note that the results from our numerical calculations indicate that except for the smallest melt polymers, the melt exhibits only partial interpenetration with the brush. For partial interpenetrations, one may assume that the volume fraction profile of the brush is of the form:[20,31]

$$\phi_b(z) = \frac{1}{2}\left[1 - \tanh\left(\frac{2(z-\tilde{\sigma})}{w}\right)\right] \tag{7}$$

where w denotes the width of the melt−brush interface and we have used $\tilde{\sigma}$ also corresponds to the height of the dry brush in nondimensional units. Using the above profile in eq 5, we obtain that the width of the interpenetration and the interfacial tensions are determined by the minimum value of the function:

$$\frac{\gamma_{PS-PMMA}N}{\rho_0 R_g} = \left[\frac{\pi^4}{36}\tilde{\sigma}w^2 + \frac{1}{w} - \frac{0.41123}{\alpha}w + \chi N\frac{w}{4}\right]_{min} \tag{8}$$

Equation 8 can be minimized in asymptotic regimes to yield,

$$\frac{\gamma_{PS-PMMA}N}{\rho_0 R_g} \simeq \begin{cases} 3/2(\pi^4/18)^{1/3}\tilde{\sigma}^{1/3}, & \tilde{\sigma} > \tilde{\sigma}^* \\ 2(\chi N/4 - 0.41/\alpha)^{1/2}, & \tilde{\sigma} < \tilde{\sigma}^* \end{cases} \tag{9}$$

where $\tilde{\sigma}^* = (18/\pi^4)(\chi N/4 - 0.41/\alpha)^{3/2}$. It may be recognized that the first case corresponds to the entropic "autophobic" regime, where the interfacial tension depends explicitly on the grafting density but not on χ. In contrast, the second case corresponds to the enthalpic regime where the interfacial tension is identical to its value between two immiscible homopolymers (compare with eq 4).

The above analysis suggests that the crossover from the "melt−brush" to "melt−melt" regimes occur for conditions involving low grafting densities, high molecular weights, and/or strong incompatibilities such that $(18/\pi^4)(\chi N/4 - 0.41/\alpha)^{3/2} \gtrsim \sigma N^{1/2}$ (note that σ here denotes the dimensional grafting density). We note that for the experimental parameters considered in this letter, $\tilde{\sigma} \simeq 2-3.5$, indicating that the enthalpic regime occurs for $\chi N \gtrsim 20$. Using a $\chi = 0.037$ for the PS−PMMA system (at 170°C), we discern that the enthalpic regime is reached for PS molecular weight of around 55 K, which is much larger than the polymers used in this study and explains the correspondence between our experimental results and the behavior expected for the melt−brush interfacial tension between chemically identical polymers.

3. Summary and Conclusions

In summary, in this article we presented experimental results quantifying the dewetting behavior of PMMA films on PS brushes. Our studies indicate a behavior similar to that expected

for autophobic dewetting situation and a dominance of entropic effects. We used strong segregation theory calculations to rationalize our observations and delineated the interplay between incompatibility and entropic effects in polymer wetting upon polymer brushes.

We comment on a few implications arising from our results for the context of functionalizing particle dispersions. In general, we observed that for commonly achieved experimental brush conditions (corresponding to $\tilde{\sigma} \simeq 2-3$ representing the height of brush in R_g units), the enthalpic incompatibility effects do not play the dominant role until very large molecular weights. Moreover, the results of Figure 4b suggests that in practice one may be able to use brushes made of incompatible polymers of sufficiently high molecular weight and achieve lower interfacial tensions (compared to brushes made of compatible polymers of small molecular weight). Because overall particle dispersability usually correlates to the melt−brush interfacial tensions, this strategy may open up the door to more functionalization possibilities when synthesis and/or grafting methods prove to be limiting.[19,22]

Acknowledgment. V.G. and V.P. were supported in part by grants from American Chemical Society Petroleum Research Fund, Robert A. Welch Foundation (F-1599), and the National Science Foundation grant 0730243. D.Y.R. was supported by KOSEF grant (2009-0067295) and the Nuclear R&D Programs funded by the Ministry of Education, Science & Technology (MEST), Korea.

References and Notes

(1) Alexander, S. *J. Phys.* **1977**, *38*, 983.
(2) DeGennes, P. G. *Macromolecules* **1980**, *13*, 1069.
(3) Milner, S. T.; Witten, T. A.; Cates, M. E. *Macromolecules* **1988**, *21*, 2610.
(4) Zhulina, Y. B.; Pryamitsyn, V. A.; Borisov, O. V. *Vysokomol. Soedin. Ser. A* **1989**, *31*, 185.
(5) Milner, S. T. *Science* **1991**, *251*, 905.
(6) Liu, Y.; Rafailaovich, M. H.; Sokolov, J.; et al.et al. *Phys. Rev. Lett.* **1994**, *73*, 440.
(7) Reiter, G.; Auroy, P.; Auvray, L. *Macromolecules* **1996**, *29*, 2150.
(8) Reiter, G.; Schultz, J.; Auroy, P.; Auvray, L. *Europhys. Lett.* **1996**, *33*, 29.
(9) Liu, Y.; Rafailovich, M. H.; Sokolov, J.; Schwarz, S. A.; Bahal, S. *Macromolecules* **1996**, *29*, 899.
(10) Henn, G.; Bucknall, D. G.; Stamm, M.; Vanhoorne, P.; Jerome, R. *Macromolecules* **1996**, *29*, 4305.
(11) Reiter, G.; Khanna, R. *Phys. Rev. Lett.* **2000**, *85*, 5599.
(12) Voronov, A.; Shafranska, O. *Langmuir* **2002**, *18*, 4471.
(13) Ge, S. R.; Guo, L. T.; Rafailovich, M. H.; Sokolov, J.; Overney, R. M.; Buenviaje, C.; Peiffer, D. G.; Schwarz, S. A. *Langmuir* **2001**, *17*, 1687.
(14) Maas, J.; Leermakers, F. A. M.; Fleer, G. J.; Stuart, M. A. C. *Langmuir* **2002**, *18*, 8871.
(15) Maas, J.; Leermakers, F. A. M.; Fleer, G. J.; Stuart, M. A. C. *Macromol. Symp.* **2003**, *191*, 69.
(16) Zhang, X. Y.; Lee, F. K.; Tsui, O. K. C. *Macromolecules* **2008**, *41*, 8148.
(17) Long, D.; Ajdari, A.; Leibler, L. *Langmuir* **1996**, *12*, 5221.
(18) Long, D.; Ajdari, A.; Leibler, L. *Langmuir* **1996**, *12*, 1675.
(19) Ferreira, P. G.; Ajdari, A.; Leibler, L. *Macromolecules* **1998**, *31*, 3994.
(20) Matsen, M. W.; Gardiner, J. M. *J. Chem. Phys.* **2001**, *115*, 2794.
(21) Matsen, M. W. *J. Chem. Phys.* **2005**, *122*, 144904.
(22) Hasegawa, R.; Aoki, Y.; Doi, M. *Macromolecules* **1996**, *29*, 6656.
(23) Borukhov, I.; Leibler, L. *Phys. Rev. E* **2000**, *62*, R41.
(24) Keddie, J. L.; Jones, R. A. L.; Cory, R. A. *Faraday Discuss.* **1994**, *98*, 219.
(25) Prucker.; et al.et al. *Macromol. Chem. Phys.* **1998**, *199*, 1435.
(26) Grohens, Y.; et al.et al. *Langmuir* **1998**, *14*, 2929.
(27) Ham, S.; Shin, C.; Kim, E.; et al.et al. *Macromolecules* **2008**, *41*, 6431.
(28) Vitt, E.; Shull, K. R. *Macromolecules* **1995**, *28*, 6349.
(29) Wyart, F. B.; Martin, P.; Redon, C. *Langmuir* **1993**, *9*, 3682.
(30) Broseta, D.; Fredrickson, G. H.; Helfand, E.; Leibler, L. *Macromolecules* **1990**, *23*, 132.
(31) Semenov, A. N. *Macromolecules* **1993**, *26*, 2273.
(32) Matsen, M. W. *J. Chem. Phys.* **2001**, *114*, 10528.
(33) Matsen, M. W.; Gardiner, J. M. *J. Chem. Phys.* **2003**, *118*, 3775.
(34) Matsen, M. W. *J. Chem. Phys.* **2004**, *121*, 1938.
(35) Russell, T. P.; Hjelm, R. P., Jr.; Seeger, P. A. *Macromolecules* **1990**, *23*, 890.